# Quark and gluon spin and orbital angular momentum in the proton

Siqi Xu,[1,2,*] Chandan Mondal,[1,2,†] Xingbo Zhao,[1,2,‡] Yang Li,[3,§] and James P. Vary[4,‖]

(BLFQ Collaboration)

[1]*Institute of Modern Physics, Chinese Academy of Sciences, Lanzhou 730000, China*
[2]*School of Nuclear Science and Technology, University of Chinese Academy of Sciences, Beijing 100049, China*
[3]*Department of Modern Physics, University of Science and Technology of China, Hefei 230026, China*
[4]*Department of Physics and Astronomy, Iowa State University, Ames, Iowa 50011, USA*

(Received 24 September 2022; accepted 28 September 2023; published 2 November 2023)

We address the proton spin puzzle with a fully relativistic and nonperturbative approach based on a light-front quantized Hamiltonian with quantum chromodynamics (QCD) input. From this, we calculate the effects from incorporating a dynamical gluon on the proton's gluon densities, helicity distribution, and orbital angular momentum that constitute the proton spin sum rule. We predict about 26% of the proton's spin is carried by the gluon's helicity and about 1.3% by its orbital angular momentum in low-momentum transfer experiments. Our approach also provides a good quality description of the proton's quark distribution functions following QCD scale evolution.

DOI: 10.1103/PhysRevD.108.094002

## I. INTRODUCTION

How the proton's spin originates from its constituents is one of the key questions in modern particle and nuclear physics. From a naive quark model, one expects that the quark spin contributes most of the proton's spin sum rule: $\frac{1}{2} = \frac{1}{2}\Delta\Sigma + \Delta G + L_q + L_g$, with quark spin $\frac{1}{2}\Delta\Sigma$, gluon spin $\Delta G$, quark orbital angular momentum (OAM) $L_q$ and gluon OAM $L_g$. However, the European Muon Collaboration experiment [1,2] discovered that quark spin contributes a small portion of the proton spin, which triggered the "proton spin crisis." It has now been determined that the quark spin contributes only around 30% to the proton's spin [3–5]. The Relativistic Heavy Ion Collider spin program has revealed that $\Delta G$ is likely sizable [3–8]. Together with the known quark spin contribution $\Delta\Sigma \sim 30\%$, the result manifests that the other terms provide the dominant fraction of the nucleon spin. Yet, there remain large uncertainties about $\Delta G$ [9]. Resolving this matter is a prime goal of future Electron-Ion Colliders (EICs) [10,11].

In this paper, we address this fundamental issue within basis light-front quantization (BLFQ), which is a fully relativistic and nonperturbative framework for solving problems in quantum field theories [12–23]. We adopt an effective light-front (LF) Hamiltonian and solve for its mass eigenstates at the scale suitable for low-resolution probes [12]. With quarks ($q$) and gluons ($g$), the Hamiltonian includes LF QCD interactions [24] relevant to the $|qqq\rangle$ and $|qqqg\rangle$ Fock sectors and a three-dimensional confinement [16]. After fitting Hamiltonian parameters to mass spectra, we compute the proton's parton distribution functions (PDFs) from the wave functions attained as eigenvectors of the Hamiltonian. We employ QCD evolution to advance from our model's low-energy scale to scales needed for comparing our results with global analyses.

The first of our two salient issues is the gluon density at a low energy scale that contributes to all the parton densities following QCD scale evolution. The second issue concerns the description of experimental data on the gluon spin contribution $\Delta G$. Similar to the scale dependence of the angular momentum observables [25,26], addressing these two issues demands a unified framework, as we demonstrate. We address the first issue by encapsulating the gluon directly into the proton at its model scale. We address the second issue by applying QCD evolution to compare with available data across various scales where we obtain agreement within sensible precision.

*xsq234@163.com
†mondal@impcas.ac.cn
‡xbzhao@impcas.ac.cn
§leeyoung1987@ustc.edu.cn
‖jvary@iastate.edu

## II. NUCLEON WAVE FUNCTIONS FROM LIGHT-FRONT QCD HAMILTONIAN

The structural information of a bound state is encoded in the light-front wave functions (LFWFs), which are obtained by solving the eigenvalue problem of the Hamiltonian: $P^-P^+|\Psi\rangle = M^2|\Psi\rangle$, where $P^\pm = P^0 \pm P^3$ defines the longitudinal momentum ($P^+$) and the LF Hamiltonian ($P^-$) of the system with $M^2$ being the mass squared eigenvalue. At fixed LF time ($x^+ = t + z = 0$), the nucleon state can be expressed as

$$|\Psi\rangle = \psi_{(qqq)}|qqq\rangle + \psi_{(qqqg)}|qqqg\rangle + \cdots, \tag{1}$$

where the $\psi_{(\ldots)}$ describe the probability amplitudes for different parton configurations in the nucleon.

At the initial scale, where the baryons are defined in terms of $|qqq\rangle$ and $|qqqg\rangle$ components, we consider the LF Hamiltonian $P^- = P^-_{\rm QCD} + P^-_C$, where $P^-_{\rm QCD}$ and $P^-_C$ are, respectively, the LF QCD Hamiltonian that incorporates interactions relevant to those leading two Fock components and a model for the confining interaction. In LF gauge, with one dynamical gluon [24],

$$\begin{aligned} P^-_{\rm QCD} = \int d^2x^\perp dx^- \Big\{ & \frac{1}{2}\bar\Phi\gamma^+ \frac{m_0^2 + (i\partial^\perp)^2}{i\partial^+}\Phi \\ & - \frac{1}{2}A^i_a[m_g^2 + (i\partial^\perp)^2]A^i_a + g_s\bar\Phi\gamma_\mu T^a A^\mu_a \Phi \\ & + \frac{1}{2}g_s^2\bar\Phi\gamma^+T^a\Phi\frac{1}{(i\partial^+)^2}\bar\Phi\gamma^+T^a\Phi\Big\}, \end{aligned} \tag{2}$$

where $\Phi$ and $A^\mu$ represent the quark and gluon fields, respectively. The variables $x^-$ and $x^\perp$ are the longitudinal and transverse position coordinates, respectively. $T$ is the generator of the $SU(3)$ gauge group in color space, and $\gamma^\mu$ are the Dirac matrices. The first and second terms in Eq. (2) are the kinetic energies of the quark and gluon with bare masses $m_0$ and $m_g$. While the gluon mass is zero in QCD, we permit an effective gluon mass to fit the nucleon form factors (FFs). The last two terms are the vertex and instantaneous interactions with coupling $g_s$. Following a Fock sector-dependent renormalization procedure developed for positronium in a basis embodying $|e\bar e\rangle$ and $|e\bar e\gamma\rangle$ [27,28] and further employed for mesons [22], we produce the quark mass counter term ($\delta m$) and define $m_0 = m_q + \delta m$, where $m_q$ is the physical quark mass. We neglect antisymmetrization of identical quarks. Referring to Ref. [29], we allow an independent quark mass $m_f$ in the vertex interaction.

We consider confinement in the leading Fock sector [16],

$$P^-_C P^+ = \frac{\kappa^4}{2}\sum_{i\neq j}\Big\{\vec r^{\,2}_{ij\perp} - \frac{\partial_{x_i}(x_i x_j \partial_{x_j})}{(m_i + m_j)^2}\Big\}, \tag{3}$$

where $\vec r_{ij\perp} = \sqrt{x_i x_j}(\vec r_{i\perp} - \vec r_{j\perp})$ is the relative coordinate related to the holographic variable [30], $\kappa$ is the strength of the confinement, and $\partial_x \equiv (\partial/\partial x)_{r_{ij\perp}}$. We omitted explicit confinement in the $|qqqg\rangle$ sector with the hope that the limited basis in the transverse direction and the massive gluon retain adequate effects of confinement. Massive gluons also appear in the Dyson-Schwinger equations (DSEs) approach as a consequence of confinement effects [31,32]. Effective gluon masses also appear in other theoretical approaches, see Ref. [33].

For the basis of BLFQ [12], we employ a plane-wave state in the longitudinal direction confined in a one-dimensional box of length $2L$ with antiperiodic (periodic) boundary conditions for quarks (gluons), two-dimensional harmonic oscillator (2D-HO) wave function, $\phi_{nm}(\vec p_\perp; b)$ with scale parameter $b$, in the transverse direction, and light-cone helicity state in the spin space [13]. Our basis choice introduces four quantum numbers for each parton single-particle state, $\bar\alpha = \{k, n, m, \lambda\}$. Here, $k$ represents the longitudinal degree of freedom that corresponds to the parton longitudinal momentum $p^+ = \frac{2\pi k}{L}$ with $k$ taking positive half-integer (integer) values for quarks (gluons). We omit the zero mode for gluons. The 2D-HO wave function carries the principal and orbital angular quantum number denoted by $n$ and $m$, respectively, and $\lambda$ represents the spin states. Note that $|qqqg\rangle$ has two color-singlet states which require one additional label to specify.

We introduce two many-parton basis space parameters. $N_{\rm max}$ is the many-parton cutoff of the 2D-HO basis states: $\sum_i (2n_i + |m_i| + 1) \le N_{\rm max}$ and $\sum_i k_i = K$. The longitudinal momentum fraction is then expressed as $x_i = k_i/K$. The resulting LFWFs with helicity $\Lambda$ in momentum space are then expressed as

$$\Psi^{\mathcal{N},\Lambda}_{\{x_i,\vec p_{\perp i},\lambda_i\}} = \sum_{\{n_i m_i\}} \psi^{\mathcal{N}}(\{\bar\alpha_i\}) \prod_{i=1}^{\mathcal{N}} \phi_{n_i m_i}(\vec p_{\perp i}, b), \tag{4}$$

with $\mathcal{N}$ being the particle number in each Fock sector and the $\psi$ are components of the eigenvectors associated with the Fock sectors $|qqq\rangle$ and $|qqqg\rangle$.

All calculations are performed with $\{N_{\rm max}, K\} = \{9, 16.5\}$. We select the HO scale parameter $b = 0.7$ GeV, UV cutoff for the instantaneous interaction $b_{\rm inst} = 3$ GeV, and set our model parameters $\{m_u, m_d, m_g, \kappa, m_f, \tilde g_s\} = \{0.31, 0.25, 0.50, 0.54, 1.80, 2.40\}$ (all are in units of GeV except $\tilde g_s$) by fitting the proton mass and electromagnetic properties. We notice that at the model scale, $\mu_0^2 = 0.24 \pm 0.01$ GeV$^2$, the probability of finding a quark in $|qqq\rangle$ is 44%, while it is 56% in $|qqqg\rangle$. Our electromagnetic radii for the proton obtained from the slope of the Sachs FFs [34–37] yields a charge radius $\sqrt{\langle r_E^2\rangle} = 0.85 \pm 0.01$ fm and a magnetic radius $\sqrt{\langle r_M^2\rangle} = 0.88 \pm 0.07$ fm, which are close to the experimentally

measured $\sqrt{\langle r_E^2\rangle_{\text{expt.}}}=0.840^{+0.003}_{-0.002}$ fm and $\sqrt{\langle r_M^2\rangle_{\text{expt.}}}=0.849^{+0.003}_{-0.003}$ fm [38]. We obtain the magnetic moment of the proton, $\mu_p = 2.443 \pm 0.027$, which is close to the experimental value $\mu_p^{\text{expt.}} = 2.79$ [39].

We also emphasize that we have model uncertainties emerging from three sources. First, in our calculation, we only consider $|qqq\rangle$ and $|qqqg\rangle$ Fock sectors and neglect the higher Fock components that incorporate additional QCD interactions. Second, we allow an independent quark mass $m_f$ as a free parameter in the vertex interaction. Third, we incorporate a phenomenological confinement in the leading Fock sector, while anticipating the massive gluon retains adequate effects of confinement in the higher Fock sector. These model uncertainties can be systematically reduced by incorporating higher Fock sectors with more dynamical gluons and sea quarks. We believe that this path forward will also reduce the need for a phenomenological confinement and a separate fermion mass for the vertex interaction. By establishing our approach for the proton in the leading two Fock sectors, $|qqq\rangle$ and $|qqqg\rangle$, we prepare a path for such future systematic improvements and a detailed analysis will be reported in future studies. In the following, we compute the effects from incorporating a dynamical gluon on the proton's valence quark and gluon densities, helicity distribution and orbital angular momentum that constitute the proton spin sum rule.

## III. PDFs

With our LFWFs, the proton's valence quarks and gluon unpolarized and helicity PDFs are

$$f(x) = \int_{\mathcal{N}} \Psi^{\mathcal{N},\Lambda}_{\{x_i,\vec{p}_{\perp i},\lambda_i\}} \Psi^{\mathcal{N},\Lambda}_{\{x_i,\vec{p}_{\perp i},\lambda_i\}} \delta(x-x_i), \tag{5}$$

$$\Delta f(x) = \int_{\mathcal{N}} \lambda_1 \Psi^{\mathcal{N},\Lambda}_{\{x_i,\vec{p}_{\perp i},\lambda_i\}} \Psi^{\mathcal{N},\Lambda}_{\{x_i,\vec{p}_{\perp i},\lambda_i\}} \delta(x-x_i), \tag{6}$$

respectively, with $f \equiv q$, $g$. We use the abbreviation $\int_{\mathcal{N}} \equiv \sum_{\mathcal{N},\lambda_i} \prod_{i=1}^{\mathcal{N}} \int [\frac{dxd^2\vec{p}_\perp}{16\pi^3}]_i 16\pi^3\ \delta(1-\sum x_j)\delta^2(\sum \vec{p}_{\perp j})$ and $i = q$, $g$ labels the valence quarks and gluon, respectively, and $\lambda_1 = 1(-1)$ for the struck parton helicity. At our model scale the PDFs for the valence quarks are normalized as $\int_0^1 q(x)dx = n_q$, with $n_q$ being the number of quarks of flavor $q$ in the proton and those PDFs together with the gluon PDF complete the momentum sum rule: $\int_0^1 \sum_i x f^i(x)dx = 1$.

To evolve our PDFs from our model scale $(\mu_0^2)$ to a higher scale $(\mu^2)$, we solve the next-to-next-to-leading order (NNLO) Dokshitzer- Gribov-Lipatov-Altarelli-Parisi (DGLAP) equations [40–42] of QCD using the Higher Order Perturbative Parton Evolution toolkit [43]. The variable $\mu$ refers to the factorization scale, which is equal to the renormalization scale in the DGLAP equation with the $\overline{\text{MS}}$ scheme. We then determine our model scale $\mu_0^2 = 0.24 \pm 0.01$ GeV$^2$ by matching the moment of our valence quark PDFs at 10 GeV$^2$ with the result from the global data fits with average values [44] $\langle x\rangle_u = 0.261 \pm 0.005$ and $\langle x\rangle_d = 0.109 \pm 0.005$.

Figure 1 shows our results for the proton unpolarized PDFs at $\mu^2 = 10$ GeV$^2$, where we compare the valence quarks and gluon distributions after QCD evolution with the NNPDF3.1 [45] and JAM [46] global fits. A similar comparison can be made with the other global fits of the quark and gluon PDFs [46–50]. We also include the proton PDFs previously obtained from a LF effective Hamiltonian [21] based on a valence Fock representation for comparison. The error bands in our evolved distributions reflect an adopted 10% uncertainty in our model scale. We find good consistency between our prediction for the proton's valence quark distributions and the global fit. Our ratio $d^v/u^v$ is also in qualitative agreement with the extracted data from the MARATHON experiment at JLab [51]. A robust method for analysing and extrapolating JLab MARATHON data results in the proton valence-quark ratio: $\lim_{x\to 1} d^v/u^v = 0.230 \pm 0.057$ [52]. We predict $d^v/u^v = 0.225 \pm 0.025$ as $x \to 1$ which agrees with the extrapolated result.

According to the Drell-Yan-West relation [53,54], at large $\mu^2$ the valence quark distributions fall off at large $x$ as $(1-x)^p$, where $p$ is associated to the number of valence quarks and for the proton $p = 3$. Our up quark unpolarized PDF falls off at large $x$ as $(1-x)^{3.2\pm0.1}$, whereas for the down quark the PDF exhibits $(1-x)^{3.5\pm0.1}$. Both agree reasonably well with the perturbative QCD prediction [55]. Our gluon PDF is suppressed at low-$x$ and moves towards

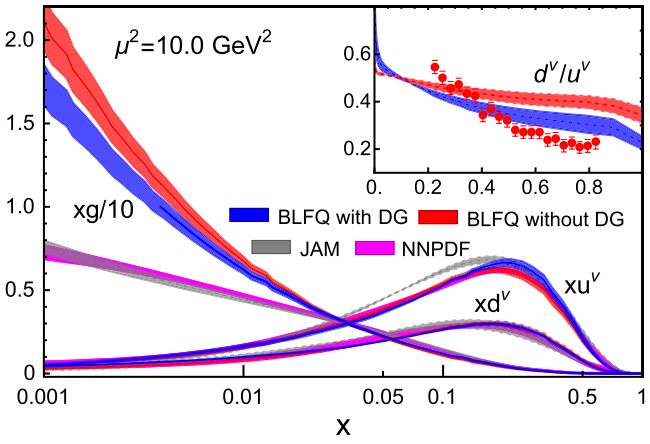


FIG. 1. The unpolarized valence quark and gluon PDFs of the proton. Our results (blue bands) obtained with one dynamical gluon are compared with the proton PDFs (pink bands) previously obtained from a LF effective Hamiltonian based on only a valence Fock representation [21] and the NNPDF3.1 [45] and JAM [46] global fits. The inset: the ratio of the valence quark PDFs is compared with the extracted data from the Jefferson Lab (JLab) MARATHON experiment [51].

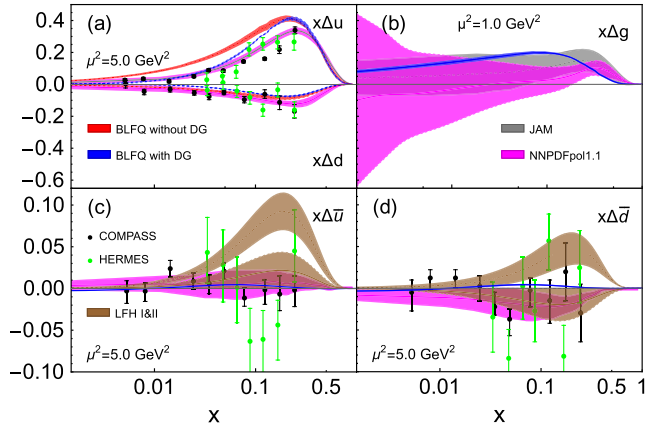


FIG. 2. The helicity PDFs of (a) the valence $u$ and $d$, (b) $g$, (c) $\bar{u}$, and (d) $\bar{d}$ in the proton. The experimental data are from COMPASS [56] and HERMES [57,58] Collaborations. The magenta band represents the global analysis by NNPDFpol1.1 [4]. The gray band in (b) corresponds to the JAM global fit [59]. The red bands in (a), (c), and (d) represent the results from a LF effective Hamiltonian in the valence-only space [21]. The sea quark distributions in (c) and (d) are compared with the predictions from light-front holographic (LFH) QCD [60].

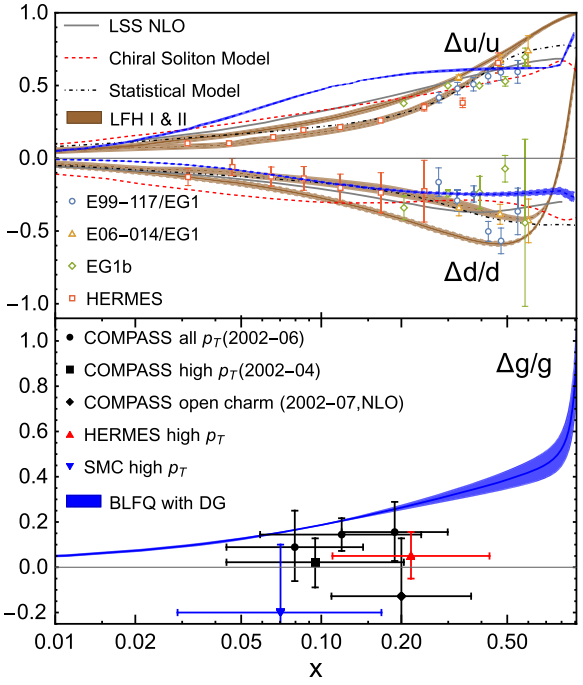


FIG. 3. Comparisons of BLFQ predictions at next-to-leading order (NLO) (blue bands) with experiments for quarks [62–64,66,67] and gluon [74–78] helicity asymmetries in the proton. The quark distributions are also compared with global analysis [57,58], predictions from LFH QCD [60] and various models [79–81].

the global fits [45,46] with our addition of a dynamical gluon, while the distribution for $x > 0.05$ is in reasonable agreement with the global fit.

Figure 2 shows the helicity PDFs of the valence up and down quark (a), gluon (b), sea up quark (c), and sea down quark (d). We find that our valence quark helicity PDFs are roughly consistent with the experimental data from COMPASS [56] and HERMES [57,58]. The $\chi^2$ per degrees of freedom (d.o.f.) for $x\Delta u$ is 24.5, whereas for the $x\Delta d$, it is 2.4. For comparison, we also include the global analysis by NNPDFpol1.1 [4] and the results previously obtained from a valence-only LF effective Hamiltonian [21]. We notice that $\Delta u(x)$ improves significantly at small-$x$ as a result of including a dynamical gluon.

In our model, the sea quarks are generated by scale evolution. We find acceptable agreement between our $\Delta\bar{u}$ and the experimental data. Note that the sea quark helicity PDFs' signs are not fixed by the experiments.

We present the gluon helicity PDF at the scale $\mu^2 = 1\ \mathrm{GeV}^2$ and we compare it with the global analyses by the JAM [59] and the NNPDF Collaborations [4]. We observe a fair agreement at small-$x$, whereas our gluon helicity distribution at large-$x$ falls faster than that of the NNPDFpol1.1 analysis. Our BLFQ prediction shows somewhat better agreement with the JAM results. Significant uncertainties exist in the large-$x$ and small-$x$ domains where even the sign is uncertain [61].

In Fig. 3, we compare the quark and gluon helicity asymmetries obtained from our BLFQ approach with data extracted from various experiments. Experimentally, the expected increase of $\Delta u/u$ is observed. Meanwhile, the down quark remains negative for $x \lesssim 0.6$ [62–68] and the global analyses favor negative values of $\Delta d/d$ at large-$x$ [3–5]. This is also supported by DSE calculations [69]. Thus, there is a tension with the pQCD constraints [55,70] and the global analyses and DSE calculations in understanding the large-$x$ behavior of the polarized PDFs. Meanwhile, the large-$x$ region, which is dominated by the valence quarks, will be tested in the JLab spin program [71–73]. The BLFQ prediction shows an acceptable agreement with the measurements [62–64,66,67] for the down quark. Our results favor the global analyses and DSE calculations [69].

We compare $\Delta g/g$ with high $p_T$ hadrons in the LO analyses [74,75] and from the open charm production in the NLO analysis [76] at COMPASS, from high $p_T$ hadrons in the LO analyses by the Spin Muon Collaboration at CERN [77] and at the HERMES experiment [78]. We find an acceptable agreement with the COMPASS data. The $\chi^2$ per d.o.f. for $\Delta g/g$ is 1.93.

The partonic helicity contributions to the proton spin are given by the first moment of the helicity distributions. At our model scale, we find the quark contribution is $\frac{1}{2}\Delta\Sigma = 0.359 \pm 0.002$ to the proton spin, with contributions $\frac{1}{2}\Delta\Sigma_u = 0.438 \pm 0.004$ and $\frac{1}{2}\Delta\Sigma_d = -0.080 \pm 0.002$. Note that $\Delta\Sigma_u$ agrees well with the world data summarized in Ref. [82], however, our $\Delta\Sigma_d$ is significantly smaller than most of the world data. We find a sizeable gluon contribution, $\Delta G = 0.131 \pm 0.003$, to the proton spin. A recent

analysis with updated data sets and PHENIX measurement [83] yielded $\Delta G = 0.2(1)$ with a constraint: $-0.7 < \Delta G < 0.5$ for $x_g \in [0.02, 0.3]$. Excluding the $x_g < 0.05$ domain, the value of $\Delta G = \int_{0.05}^{0.2} dx \Delta g(x) = 0.23(6)$ [4] and $\Delta G = \int_{0.05}^{1} dx \Delta g(x) = 0.19(6)$ [7] were extracted. The lattice QCD simulations predicted $\Delta G = 0.251(47)(16)$ at the physical pion mass [84]. Future measurements of $\Delta g(x)$ in the $x_g < 0.02$ are required to decrease the uncertainty in $\Delta G$. Fortunately, the upcoming EICs [10,11,85] aim to accurately measure the gluon helicity distribution, particularly in the small-$x$ region.

## IV. ORBITAL ANGULAR MOMENTUM

We find a sizeable canonical orbital angular momentum (OAM) contribution to the proton spin using generalized transverse momentum dependent distributions (GTMDs) as [86–88]

$$L_z^i = -\int \mathrm{d}x \mathrm{d}^2\vec{p}_\perp \frac{\vec{p}_\perp^2}{M^2} F_{1,4}^i(x, 0, \vec{p}_\perp^2, 0, 0), \tag{7}$$

with $F_{1,4}^i(x, \xi, \vec{p}_\perp^2, \vec{p}_\perp \cdot \vec{q}_\perp, \vec{q}_\perp^2)$ being one of the GTMDs for the unpolarized parton [89–91], where $q$ is the momentum transfer and the skewness variable $\xi$ represents the momentum transfer in the longitudinal direction, and $M$ is the proton mass. With $\epsilon_\perp^{12} = 1$ the GTMD can be expressed as

$$F_{1,4}^i = \sum_\Lambda \int_\mathcal{N} \frac{-iM^2}{2(\epsilon_\perp^{ij} \vec{p}_\perp^{\,i} \vec{q}_\perp^{\,j})} \Lambda \Psi^{\Lambda *}_{\{x_i', \vec{p}_{i\perp}', \lambda_i\}} \Psi^{\Lambda}_{\{x_i, \vec{p}_{i\perp}, \lambda_i\}} \times \delta^2\left(\vec{p}_\perp - \frac{\vec{p}_{i\perp}' + \vec{p}_{i\perp}}{2}\right) \delta(x - x_i). \tag{8}$$

We predict that $L_z^u = 0.0327 \pm 0.0013$, $L_z^d = -0.0114 \pm 0.0004$, and $L_z^g = -0.0065 \pm 0.0005$ consistent with light-cone quark models [86]. Note that nothing is known about $L(x)$ experimentally. Our calculation provides predictions for the quark and gluon helicities and their OAM from the future experiments as well as baselines for theoretical investigations with higher Fock components.

## V. CONCLUSION AND OUTLOOK

Using BLFQ, we have solved for the first time the light-front QCD Hamiltonian for the proton within the combined constituent three quarks ($|qqq\rangle$) and three quarks and one gluon ($|qqqg\rangle$) Fock spaces. The resulting LFWFs obtained from this Hamiltonian were employed to compute the proton PDFs.

We have calculated the quark and gluon helicity distributions and their OAM that constitutes the proton spin sum rule. We have observed a qualitative agreement between our predictions for the polarized distributions and the experimental data and/or the global fits. Our model leads to somewhat less satisfactory results for $\Delta q(x)$ when we compare with the experimental data. However, it is reasonable at this stage since it can be systematically improved. Note that the contribution of an additional $q\bar{q}$ pair, which is relevant at larger distances and embodies the pion cloud in the proton, likely plays an important role in reproducing the experimental data for the polarized quark distributions. From the theory-data comparison, we find that the BLFQ prediction for $\Delta d/d$ is consistent with existing experimental data and global fits and remains negative at large-$x$. This key property of the proton will be tested very soon in upcoming experiments. Further, our work provides a prediction of the expected data for the gluon polarized PDF from future experiments as well as a guidance for the theoretical investigations of this PDF. Comparing theory and experimental data for $\Delta g/g$ available in the small-$x$ region, we find an acceptable agreement with the COMPASS data considering the large experimental uncertainties. It seems reasonable that our prediction thereby provides guidance for the gluon helicity PDF in the large-$x$ domain, where our result agrees with the perturbative QCD constraint.

With one dynamical gluon, we have predicted that $\Delta G$ contributes $26.0 \pm 0.6\%$, while the contribution from $\Delta\Sigma$ is $72.0 \pm 0.4\%$ to the proton spin. The contributions from the OAM are: $L_z^u = 0.0327 \pm 0.0013$, $L_z^d = -0.0114 \pm 0.0004$, and $L_z^g = -0.0065 \pm 0.0005$. Experimentally, there remain large uncertainties in $\Delta g(x)$, including the sign in the small-$x$ domain. Future measurements of $\Delta g(x)$ for $x_g < 0.02$ would be valuable to constrain $\Delta G$. On the other hand, nothing is experimentally known about OAM. Discovering these properties represents major goals of EICs [10,11].

The PDFs at a higher scale have been generated based on the NNLO DGLAP equations and we find reasonable agreement with the global fits for the unpolarized valence quark and gluon distributions. We have predicted that $d^v/u^v = 0.225 \pm 0.025$ at $x \to 1$ which agrees with the recent analysis from the MARATHON experiment yielding $\lim_{x\to 1} d^v/u^v = 0.230 \pm 0.057$ [52].

The present calculations can be viewed as a brief report of some first results. The obtained LFWFs can be further employed to compute the quark and gluon Generalized Parton distribution functions, Transverse-momentum dependent Parton distribution functions, and Wigner distributions as well as the double parton correlations, etc., in the nucleon. The present calculation can be straightforwardly extended to higher Fock sectors to incorporate, for example, sea quarks and multigluon configurations.

## ACKNOWLEDGMENTS

C. M. is supported by new faculty start up funding by the Institute of Modern Physics, Chinese Academy of Sciences, Grant No. E129952YR0. C. M. also thanks the Chinese Academy of Sciences Presidents International Fellowship

Initiative for the support via Grant No. 2021PM0023. X. Z. is supported by new faculty startup funding by the Institute of Modern Physics, Chinese Academy of Sciences, by Key Research Program of Frontier Sciences, Chinese Academy of Sciences, Grant No. ZDBS-LY-7020, by the Natural Science Foundation of Gansu Province, China, Grant No. 20JR10RA067, by the Foundation for Key Talents of Gansu Province, by the Central Funds Guiding the Local Science and Technology Development of Gansu Province, Grant No. 22ZY1QA006, by Gansu International Collaboration and Talents Recruitment Base of Particle Physics (2023–2027), by International Partnership Program of the Chinese Academy of Sciences, Grant No. 016GJHZ2022103FN, by National Natural Science Foundation of China, Grant No. 12375143 and by the Strategic Priority Research Program of the Chinese Academy of Sciences, Grant No. XDB34000000. Y. L. is supported by the new faculty startup fund of University of Science and Technology of China, by the National Natural Science Foundation of China (NSFC) under Grant No. 12375081, and by the Chinese Academy of Sciences under Grant No. YSBR-101. J. P. V. is supported by the U.S. Department of Energy under Grants No. DE-SC0023692, and No. DE-SC0023707. This research used resources of the National Energy Research Scientific Computing Center (NERSC), a U.S. Department of Energy Office of Science User Facility operated under Contract No. DE-AC02- 05CH11231. A portion of the computational resources were also provided by Gansu Computing Center.

[1] J. Ashman *et al.* (European Muon Collaboration), A measurement of the spin asymmetry and determination of the structure function g(1) in deep inelastic muon-proton scattering, Phys. Lett. B **206**, 364 (1988).
[2] J. Ashman *et al.* (European Muon Collaboration), An investigation of the spin structure of the proton in deep inelastic scattering of polarized muons on polarized protons, Nucl. Phys. **B328**, 1 (1989).
[3] D. de Florian, R. Sassot, M. Stratmann, and W. Vogelsang, Extraction of spin-dependent parton densities and their uncertainties, Phys. Rev. D **80**, 034030 (2009).
[4] E. R. Nocera, R. D. Ball, S. Forte, G. Ridolfi, and J. Rojo (NNPDF Collaboration), A first unbiased global determination of polarized PDFs and their uncertainties, Nucl. Phys. **B887**, 276 (2014).
[5] J. J. Ethier, N. Sato, and W. Melnitchouk, First simultaneous extraction of spin-dependent parton distributions and fragmentation functions from a global QCD analysis, Phys. Rev. Lett. **119**, 132001 (2017).
[6] L. Adamczyk *et al.* (STAR Collaboration), Precision measurement of the longitudinal double-spin asymmetry for inclusive jet production in polarized proton collisions at $\sqrt{s} = 200$ GeV, Phys. Rev. Lett. **115**, 092002 (2015).
[7] D. de Florian, R. Sassot, M. Stratmann, and W. Vogelsang, Evidence for polarization of gluons in the proton, Phys. Rev. Lett. **113**, 012001 (2014).
[8] M. S. Abdallah *et al.* (STAR Collaboration), Longitudinal double-spin asymmetry for inclusive jet and dijet production in polarized proton collisions at $\sqrt{s} = 510$ GeV, Phys. Rev. D **105**, 092011 (2022).
[9] X. Ji, F. Yuan, and Y. Zhao, What we know and what we don't know about the proton spin after 30 years, Nat. Rev. Phys. **3**, 27 (2021).
[10] R. Abdul Khalek, A. Accardi, J. Adam, D. Adamiak, W. Akers, M. Albaladejo, A. Al-bataineh, M. G. Alexeev, F. Ameli, P. Antonioli *et al.*, Science requirements and detector concepts for the electron-ion collider: EIC Yellow Report, Nucl. Phys. **A1026**, 122447 (2022).
[11] D. P. Anderle, V. Bertone, X. Cao, L. Chang, N. Chang, G. Chen, X. Chen, Z. Chen, Z. Cui, L. Dai *et al.*, Electron-ion collider in China, Front. Phys. (Beijing) **16**, 64701 (2021).
[12] J. P. Vary, H. Honkanen, J. Li, P. Maris, S. J. Brodsky, A. Harindranath, G. F. de Teramond, P. Sternberg, E. G. Ng, and C. Yang, Hamiltonian light-front field theory in a basis function approach, Phys. Rev. C **81**, 035205 (2010).
[13] X. Zhao, H. Honkanen, P. Maris, J. P. Vary, and S. J. Brodsky, Electron g-2 in light-front quantization, Phys. Lett. B **737**, 65 (2014).
[14] S. Nair, C. Mondal, X. Zhao, A. Mukherjee, and J. P. Vary (BLFQ Collaboration), Basis light-front quantization approach to photon, Phys. Lett. B **827**, 137005 (2022).
[15] P. Wiecki, Y. Li, X. Zhao, P. Maris, and J. P. Vary, Basis light-front quantization approach to positronium, Phys. Rev. D **91**, 105009 (2015).
[16] Y. Li, P. Maris, X. Zhao, and J. P. Vary, Heavy quarkonium in a holographic basis, Phys. Lett. B **758**, 118 (2016).
[17] S. Jia and J. P. Vary, Basis light front quantization for the charged light mesons with color singlet Nambu–Jona-Lasinio interactions, Phys. Rev. C **99**, 035206 (2019).
[18] S. Tang, Y. Li, P. Maris, and J. P. Vary, Heavy-light mesons on the light front, Eur. Phys. J. C **80**, 522 (2020).
[19] J. Lan, C. Mondal, S. Jia, X. Zhao, and J. P. Vary, Parton distribution functions from a light front Hamiltonian and QCD evolution for light mesons, Phys. Rev. Lett. **122**, 172001 (2019).
[20] C. Mondal, S. Xu, J. Lan, X. Zhao, Y. Li, D. Chakrabarti, and J. P. Vary, Proton structure from a light-front Hamiltonian, Phys. Rev. D **102**, 016008 (2020).
[21] S. Xu, C. Mondal, J. Lan, X. Zhao, Y. Li, J. P. Vary (BLFQ Collaboration), Nucleon structure from basis light-front quantization, Phys. Rev. D **104**, 094036 (2021).

[22] J. Lan, K. Fu, C. Mondal, X. Zhao, and J. P. Vary (BLFQ Collaboration), Light mesons with one dynamical gluon on the light front, Phys. Lett. B **825**, 136890 (2022).
[23] Z. Kuang, K. Serafin, X. Zhao, and J. P. Vary, All-charm tetraquark in front form dynamics, Phys. Rev. D **105**, 094028 (2022).
[24] S. J. Brodsky, H. C. Pauli, and S. S. Pinsky, Quantum chromodynamics and other field theories on the light cone, Phys. Rep. **301**, 299 (1998).
[25] A. W. Thomas, Interplay of spin and orbital angular momentum in the proton, Phys. Rev. Lett. **101**, 102003 (2008).
[26] S. Jia and F. Huang, Scale dependencies of proton spin constituents with a nonperturbative alphas, Phys. Rev. D **86**, 094035 (2012).
[27] X. Zhao, Advances in basis light-front quantization, Few Body Syst. **56**, 257 (2015).
[28] X. Zhao, K. Fu, H. Zhao, and J. P. Vary, Positronium: An illustration of nonperturbative renormalization in a basis light-front approach, Proc. Sci., LC2019 (**2020**) 090 [arXiv:2103.06719].
[29] S. D. Glazek and R. J. Perry, Special example of relativistic Hamiltonian field theory, Phys. Rev. D **45**, 3740 (1992).
[30] S. J. Brodsky, G. F. de Teramond, H. G. Dosch, and J. Erlich, Light-front holographic QCD and emerging confinement, Phys. Rep. **584**, 1 (2015).
[31] J. M. Cornwall, Dynamical mass generation in continuum QCD, Phys. Rev. D **26**, 1453 (1982).
[32] R. Alkofer and L. von Smekal, The infrared behavior of QCD Green's functions: Confinement dynamical symmetry breaking, and hadrons as relativistic bound states, Phys. Rep. **353**, 281 (2001).
[33] A. Deur, S. J. Brodsky, and G. F. de Teramond, The QCD running coupling, Prog. Part. Nucl. Phys. **90**, 1 (2016).
[34] G. D. Cates, C. W. de Jager, S. Riordan, and B. Wojtsekhowski, Flavor decomposition of the elastic nucleon electromagnetic FFs, Phys. Rev. Lett. **106**, 252003 (2011).
[35] I. A. Qattan and J. Arrington, Flavor decomposition of the nucleon electromagnetic FFs, Phys. Rev. C **86**, 065210 (2012).
[36] M. Diehl and P. Kroll, Nucleon FFs, generalized parton distributions and quark angular momentum, Eur. Phys. J. C **73**, 2397 (2013).
[37] F. J. Ernst, R. G. Sachs, and K. C. Wali, Electromagnetic form factors of the nucleon, Phys. Rev. **119**, 1105 (1960).
[38] Y. H. Lin, H. W. Hammer, and U. G. Meißner, New insights into the nucleon's electromagnetic structure, Phys. Rev. Lett. **128**, 052002 (2022).
[39] M. Tanabashi *et al.* (Particle Data Group Collaboration), Review of particle physics, Phys. Rev. D **98**, 030001 (2018).
[40] Y. L. Dokshitzer, Calculation of the structure functions for deep inelastic scattering and $e+$ $e-$ annihilation by perturbation theory in quantum chromodynamics, Zh. Eksp. Teor. Fiz. **73**, 1216 (1977) [Sov. Phys. JETP **46**, 641 (1977)].
[41] V. N. Gribov and L. N. Lipatov, Deep inelastic e p scattering in perturbation theory, Sov. J. Nucl. Phys. **15**, 438 (1972).
[42] G. Altarelli and G. Parisi, Asymptotic freedom in Parton language, Nucl. Phys. **B126**, 298 (1977).
[43] G. P. Salam and J. Rojo, A higher order perturbative parton evolution toolkit (HOPPET), Comput. Phys. Commun. **180**, 120 (2009).
[44] G. F. de Teramond, T. Liu, R. S. Sufian, H. G. Dosch, S. J. Brodsky, and A. Deur (HLFHS Collaboration), Universality of generalized parton distributions in light-front holographic QCD, Phys. Rev. Lett. **120**, 182001 (2018).
[45] R. D. Ball *et al.* (NNPDF Collaboration), Parton distributions from high-precision collider data, Eur. Phys. J. C **77**, 663 (2017).
[46] E. Moffat, W. Melnitchouk, T. C. Rogers, and N. Sato (Jefferson Lab Angular Momentum (JAM) Collaboration), Simultaneous Monte Carlo analysis of parton densities and fragmentation functions, Phys. Rev. D **104**, 016015 (2021).
[47] T. J. Hou, J. Gao, T. J. Hobbs, K. Xie, S. Dulat, M. Guzzi, J. Huston, P. Nadolsky, J. Pumplin, C. Schmidt *et al.*, New CTEQ global analysis of quantum chromodynamics with high-precision data from the LHC, Phys. Rev. D **103**, 014013 (2021).
[48] A. Accardi, L. T. Brady, W. Melnitchouk, J. F. Owens, and N. Sato, Constraints on large-$x$ parton distributions from new weak boson production and deep-inelastic scattering data, Phys. Rev. D **93**, 114017 (2016).
[49] S. Bailey, T. Cridge, L. A. Harland-Lang, A. D. Martin, and R. S. Thorne, Parton distributions from LHC, HERA, Tevatron and fixed target data: MSHT20 PDFs, Eur. Phys. J. C **81**, 341 (2021).
[50] H. Abramowicz *et al.* (H1 and ZEUS Collaborations), Combination of measurements of inclusive deep inelastic $e^{\pm}p$ scattering cross sections and QCD analysis of HERA data, Eur. Phys. J. C **75**, 580 (2015).
[51] D. Abrams *et al.* (Jefferson Lab Hall A Tritium Collaboration), Measurement of the nucleon $F_2^n/F_2^p$ structure function ratio by the Jefferson Lab MARATHON tritium/helium-3 deep inelastic scattering experiment, Phys. Rev. Lett. **128**, 132003 (2022).
[52] Z. F. Cui, F. Gao, D. Binosi, L. Chang, C. D. Roberts, and S. M. Schmidt, Valence quark ratio in the proton, Chin. Phys. Lett. **39**, 041401 (2022).
[53] S. D. Drell and T. M. Yan, Connection of elastic electromagnetic nucleon form-factors at large Q**2 and deep inelastic structure functions near threshold, Phys. Rev. Lett. **24**, 181 (1970).
[54] G. B. West, Phenomenological model for the electromagnetic structure of the proton, Phys. Rev. Lett. **24**, 1206 (1970).
[55] S. J. Brodsky, M. Burkardt, and I. Schmidt, Perturbative QCD constraints on the shape of polarized quark and gluon distributions, Nucl. Phys. **B441**, 197 (1995).
[56] M. G. Alekseev *et al.* (COMPASS Collaboration), Quark helicity distributions from longitudinal spin asymmetries in muon-proton and muon-deuteron scattering, Phys. Lett. B **693**, 227 (2010).
[57] A. Airapetian *et al.* (HERMES Collaboration), Flavor decomposition of the sea quark helicity distributions in the nucleon from semiinclusive deep inelastic scattering, Phys. Rev. Lett. **92**, 012005 (2004).
[58] A. Airapetian *et al.* (HERMES Collaboration), Quark helicity distributions in the nucleon for up, down, and strange quarks from semi-inclusive deep-inelastic scattering, Phys. Rev. D **71**, 012003 (2005).
[59] N. Sato, W. Melnitchouk, S. E. Kuhn, J. J. Ethier, and A. Accardi (Jefferson Lab Angular Momentum Collaboration),

Iterative Monte Carlo analysis of spin-dependent parton distributions, Phys. Rev. D **93**, 074005 (2016).
[60] T. Liu, R. S. Sufian, G. F. de Téramond, H. G. Dosch, S. J. Brodsky, and A. Deur, Unified description of polarized and unpolarized quark distributions in the proton, Phys. Rev. Lett. **124**, 082003 (2020).
[61] Y. Zhou, N. Sato, and W. Melnitchouk (Jefferson Lab Angular Momentum (JAM) Collaboration), How well do we know the gluon polarization in the proton?, Phys. Rev. D **105**, 074022 (2022).
[62] X. Zheng *et al.* (Jefferson Lab Hall A Collaboration), Precision measurement of the neutron spin asymmetry A1**N and spin flavor decomposition in the valence quark region, Phys. Rev. Lett. **92**, 012004 (2004).
[63] X. Zheng *et al.* (Jefferson Lab Hall A Collaboration), Precision measurement of the neutron spin asymmetries and spin-dependent structure functions in the valence quark region, Phys. Rev. C **70**, 065207 (2004).
[64] D. S. Parno *et al.* (Jefferson Lab Hall A Collaboration), Precision measurements of $A_1^n$ in the deep inelastic regime, Phys. Lett. B **744**, 309 (2015).
[65] K. V. Dharmawardane *et al.* (CLAS Collaboration), Measurement of the x- and Q**2-dependence of the asymmetry A(1) on the nucleon, Phys. Lett. B **641**, 11 (2006).
[66] A. Airapetian *et al.* (HERMES Collaboration), Flavor decomposition of the sea quark helicity distributions in the nucleon from semiinclusive deep inelastic scattering, Phys. Rev. Lett. **92**, 012005 (2004).
[67] A. Airapetian *et al.* (HERMES Collaboration), Quark helicity distributions in the nucleon for up, down, and strange quarks from semi-inclusive deep-inelastic scattering, Phys. Rev. D **71**, 012003 (2005).
[68] M. G. Alekseev *et al.* (COMPASS Collaboration), Quark helicity distributions from longitudinal spin asymmetries in muon-proton and muon-deuteron scattering, Phys. Lett. B **693**, 227 (2010).
[69] C. D. Roberts, R. J. Holt, and S. M. Schmidt, Nucleon spin structure at very high-x, Phys. Lett. B **727**, 249 (2013).
[70] H. Avakian, S. J. Brodsky, A. Deur, and F. Yuan, Effect of orbital angular momentum on valence-quark helicity distributions, Phys. Rev. Lett. **99**, 082001 (2007).
[71] JLab experiment E12-06-109, spokespersons: S. Kuhn (contact), S. Bultmann, A. Deur, V. Dharmawardane, K. Griffioen, M. Holtrop, Y. Prok, D. Crabb, and T. Forest, https://www.jlab.org/exp prog/proposals/ proposal updates/ PR12-06-109 pac36.pdf.
[72] 74JLab experiment E12-06-110, spokespersons: X. Zheng (contact), G. Cates, J.-P. Chen, and Z.-E. Meziani, https://www.jlab.org/exp_prog/proposals/06/PR12-06-110.pdf.
[73] JLab experiment E12-06-122, spokespersons: B. Wojtsekhowski (contact), J. Annand, T. Averett, G. Cates, N. Liyanage, G. Rosner, and X. Zheng, https://www.jlab.org/exp-prog/12GEV-EXP/E1206122.html.
[74] E. S. Ageev *et al.* (COMPASS Collaboration), Gluon polarization in the nucleon from quasi-real photoproduction of high-p(T) hadron pairs, Phys. Lett. B **633**, 25 (2006).
[75] C. Adolph *et al.* (COMPASS Collaboration), Leading-order determination of the gluon polarisation from semi-inclusive deep inelastic scattering data, Eur. Phys. J. C **77**, 209 (2017).
[76] C. Adolph *et al.* (COMPASS Collaboration), Leading and next-to-leading order gluon polarization in the nucleon and longitudinal double spin asymmetries from open charm muoproduction, Phys. Rev. D **87**, 052018 (2013).
[77] B. Adeva *et al.* (Spin Muon (SMC) Collaboration), Spin asymmetries for events with high p(T) hadrons in DIS and an evaluation of the gluon polarization, Phys. Rev. D **70**, 012002 (2004).
[78] A. Airapetian *et al.* (HERMES Collaboration), Leading-order determination of the gluon polarization from high-p(T) hadron electroproduction, J. High Energy Phys. 08 (2010) 130.
[79] E. Leader, A. V. Sidorov, and D. B. Stamenov, A New evaluation of polarized parton densities in the nucleon, Eur. Phys. J. C **23**, 479 (2002).
[80] M. Wakamatsu, Light flavor sea quark distributions in the nucleon in the SU(3) chiral quark soliton model. 1. Phenomenological predictions, Phys. Rev. D **67**, 034005 (2003).
[81] C. Bourrely, J. Soffer, and F. Buccella, A Statistical approach for polarized parton distributions, Eur. Phys. J. C **23**, 487 (2002).
[82] A. Deur, S. J. Brodsky, and G. F. De Téramond, The spin structure of the nucleon, Rep. Prog. Phys. **82**, 076201 (2019).
[83] A. Adare *et al.* (PHENIX Collaboration), The polarized gluon contribution to the proton spin from the double helicity asymmetry in inclusive pi0 production in polarized $p+p$ collisions at $s**(1/2) = 200$-GeV, Phys. Rev. Lett. **103**, 012003 (2009).
[84] Y. B. Yang, R. S. Sufian, A. Alexandru, T. Draper, M. J. Glatzmaier, K. F. Liu, and Y. Zhao, Glue spin and helicity in the proton from lattice QCD, Phys. Rev. Lett. **118**, 102001 (2017).
[85] A. Accardi, J. L. Albacete, M. Anselmino, N. Armesto, E. C. Aschenauer, A. Bacchetta, D. Boer, W. K. Brooks, T. Burton, N. B. Chang *et al.*, Electron ion collider: The next QCD frontier: Understanding the glue that binds us all, Eur. Phys. J. A **52**, 268 (2016).
[86] C. Lorce and B. Pasquini, Quark Wigner distributions and orbital angular momentum, Phys. Rev. D **84**, 014015 (2011).
[87] S. Bhattacharya, R. Boussarie, and Y. Hatta, Signature of the gluon orbital angular momentum, Phys. Rev. Lett. **128**, 182002 (2022).
[88] Y. Liu, S. Xu, C. Mondal, X. Zhao, and J. P. Vary (BLFQ Collaboration), Angular momentum and generalized parton distributions for the proton with basis light-front quantization, Phys. Rev. D **105**, 094018 (2022).
[89] S. Meissner, A. Metz, and M. Schlegel, Generalized parton correlation functions for a spin-1/2 hadron, J. High Energy Phys. 08 (2009) 056.
[90] C. Lorcé and B. Pasquini, Structure analysis of the generalized correlator of quark and gluon for a spin-1/2 target, J. High Energy Phys. 09 (**2013**) 138.
[91] S. Bhattacharya, A. Metz, and J. Zhou, Generalized TMDs and the exclusive double Drell–Yan process, Phys. Lett. B **771**, 396 (2017); **810**, 135866(E) (2020).